

# Combining Multisensor Satellite Remote Sensing Time Series to Assess Disturbances in Central European Temperate Forests

SIMON KÖNIG<sup>1,2,3</sup>, FRANK THONFELD<sup>4,5</sup>, OLENA DUBOVYK<sup>1,6</sup> & MARCO HEURICH<sup>2,3,7</sup>

*Abstract: Bark Beetle outbreaks are an important disturbance agent in Central European forests, with strong impacts in recent years. Here, dense time series of Landsat, Sentinel-2, and Sentinel-1, plus their combinations, were used to detect bark beetle infestations in the Bavarian Forest National Park, Germany. Various processing steps were applied to all data, and a consistent data cube was built, of which a variety of parameters were computed. The parameters with the best ability to separate infested from healthy plots were selected for the detection. From these, infestation probability time series were derived and classified into infested/healthy according to increasing probability thresholds, and the respective detections were evaluated. The results show that Sentinel-2 works best, both in terms of spatial accuracy and an early detection. Combining Sentinel-2 and Landsat didn't provide benefits, and Sentinel-2 SAR data or the fusion of SAR and multispectral data performed worse. The results of this study have important implications for forest monitoring and management.*

## 1 Introduction

Temperate forests are a major part of the biosphere, hosts of biodiversity, and an important component of land-atmosphere interactions. If healthy and intact, they serve as net carbon sinks, and thus are a key asset in the mitigation of climate change. Besides, they provide a variety of ecosystem services to humankind, including the provision of goods such as timber, regulating effects like the protection against erosion, or cultural services such as the potential for recreation (BROCKERHOFF et al. 2017). Natural disturbances are crucial for the dynamics of temperate forest ecosystems. This includes both abiotic (e.g. windthrow, drought) and biotic disturbances (e.g. insect outbreaks, pathogens). By changing the structure, composition, and function of forests, they facilitate succession, renewal, and reorganization. Thus, they contribute to forest heterogeneity, biodiversity, and resilience (SEIDL et al. 2017). In recent decades, disturbance regimes have changed around the globe, whereby many of these changes can be attributed to climate change.

---

<sup>1</sup> Geographisches Institut, Universität Bonn, Meckenheimer Allee 156, 53115 Bonn

<sup>2</sup> Nationalpark Bayerischer Wald, Freyunger Straße 2, 94481 Grafenau, E-Mail: [simon.koenig, marco.heurich]@npv-bw.bayern.de

<sup>3</sup> Fakultät für Umwelt und Natürliche Ressourcen, Universität Freiburg, Tennenbacher Straße 4, 79106 Freiburg

<sup>4</sup> Deutsches Fernerkundungsdatenzentrum, Deutsches Zentrum für Luft- und Raumfahrt, Münchener Straße 20, 82234 Weßling, E-Mail: frank.thonfeld@dlr.de

<sup>5</sup> Institut für Geographie und Geologie, Universität Würzburg, Am Hubland, 97074 Würzburg

<sup>6</sup> Zentrum für Fernerkundung der Landoberfläche, Universität Bonn, Genscherallee 3, 53113 Bonn, E-Mail: odubovyk@uni-bonn.de

<sup>7</sup> Department of Forestry and Wildlife Management, Inland Norway University of Applied Sciences, Anne Evenstads Veg 80, 2480 Koppang, Norwegen

Likewise, further shifts in forest disturbance regimes are to be expected under further warming climate, potentially resulting in so-called “megadisturbances” which may alter temperate forest ecosystems beyond their resilience (MILLAR & STEPHENSON 2015; SEIDL et al. 2017).

Outbreaks of bark beetles are one of the most important disturbance agents in temperate forests. These insects reproduce under the bark of their host trees. By feeding on the tree’s phloem, i.e. the living tissue under the bark, many bark beetle species disrupt water and nutrient transport and consequently kill their host tree (HLÁSNY et al. 2021). In Central Europe, the bark beetle species whose outbreaks have historically caused the most widespread consequences is the European Spruce Bark Beetle (*Ips typographus* L.). In recent years, facilitated by a series of hot and dry summers and past forest practice resulting in widespread old-growth Norway Spruce (*Picea abies* L.), i.e. the main host tree of the European Spruce Bark Beetle, Central Europe has experienced bark beetle-induced tree mortality levels beyond any historical level. For example, 16 % of all spruce growing stock have been subject to die-off between 2018 in 2020 in Germany alone (BUNDESMINISTERIUM FÜR ERNÄHRUNG UND LANDWIRTSCHAFT 2021).

Satellite remote sensing has been proven to be a highly valuable tool in the monitoring of forest disturbances, very much including bark beetle infestations (SENF et al. 2017). Bark beetle disturbances happen in three distinct stages: during the *green attack* phase, the tree foliage does not visibly change. This changes in the second, i.e. *red attack* phase: as the die-off of the tree proceeds, its needles first turn yellow and then proceed to a red color. As time progresses, the tree starts to lose its needles and the tree bark slowly starts to detach. This constitutes the *grey attack* phase. The detection of dead trees in the grey attack phase is relatively easy using satellite imagery (WULDER et al. 2006). However, the early detection of infested trees at the beginning of the red attack or even in the green attack phase is more challenging while at the same time very important, because in managed forests, infested trees should be logged and removed quickly to prevent further spread. Bark beetle infestations induce physiological changes in a tree, including loss of water and chlorophyll content in the needles, but these changes induce only subtle shifts in the reflectance, at least in the beginning of an infestation (ABDULLAH et al. 2018). A variety of approaches exist for the detection of bark beetle infestations. Many of these relied on multispectral data, e.g. from Landsat and Sentinel-2 (ABDULLAH et al. 2019; BÁRTA et al. 2021; HAIS & KUČERA 2008; MEIGS et al. 2011). SAR imagery from sensors such as Sentinel-1 or TerraSAR-X has only seldomly been applied (HOLLAUS & VREUGDENHIL 2019). In addition, approaches using high time series density have not frequently been applied (BÁRTA et al. 2021; HUO et al. 2021), even though a high observation density is beneficial to ensure an early detection of bark beetle infestations (SENF et al. 2017). The same holds true for the combination of different kinds of data to increase the density of applied time series, which is especially important for forestry applications in cloud-poor regions (REICHE et al. 2018). This study tries to close these gaps by using full time series of multiple satellites. Its goal is to assess how well data of different sensors, as well as their combinations, can be used to detect bark beetle infestations. This refers to both the spatial accuracy of detection as well as the date on which a detection happens. Assessing the capabilities of dense time series as well as such derived from multiple satellites is crucial for a potential future development of large-scale near-realtime bark beetle infestation monitoring systems.

## 2 Data and Methods

### 2.1 Study Area

The Bavarian Forest National Park in Southeastern Germany served as a study area for the approach. Founded in 1970, Germany's oldest National Park comprises an area of ca. 250 km<sup>2</sup>. The park is located at altitudes between 600 and 1450 m and largely dominated by coniferous forests (HEURICH et al. 2010). Mostly characterized by old-growth Norway, the park has strongly been affected by disturbances of the European Spruce Bark Beetle. In the park's core zone, infested trees are not cleared, which enables the longterm monitoring of bark beetle outbreaks (LATIFI et al. 2021). Yearly infested areas in the park have been documented in a spatially explicit manner based on aerial imagery since 1988 (HEURICH et al. 2010). This is a unique dataset that served as a reference dataset for this study.

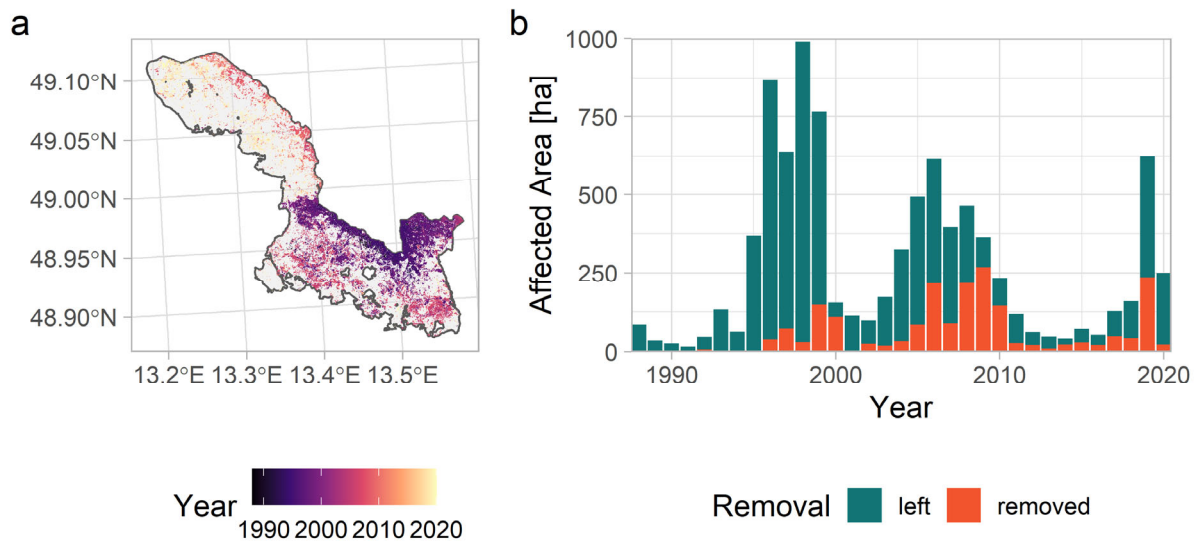


Fig. 1: Overview of bark beetle disturbances in the Bavarian Forest National Park. a) shows a map of all disturbances in the National Park since the 1980s. b) is a summary of the total area infested per year

### 2.2 Satellite Data

The following satellite data was used: the Landsat satellite family, providing data since 1982 with a spatial resolution of 30 m, as well as Sentinel-2, providing data since 2015 with a spatial resolution of 10 to 20 m, were used as sources of multispectral imagery, whereby Landsat has a repeat interval of 16 days, and Sentinel-2 offers a three-day revisit. Sentinel-1 was included as well, delivering SAR data with a spatial resolution of approximately 10 m and a revisit of six days. In total, 3177 multispectral and 1081 SAR images were used.

## 2.3 Methods

### 2.3.1 Data Processing

Since one major goal of this study was to compare and combine multiple kinds of satellite data, a first important step was the generation of analysis-ready data (ARD) to ensure that all data can be used in conjunction. Therefore, extensive processing steps were applied to both the multispectral and the SAR data. Landsat and Sentinel-2, besides their differences regarding spatial and temporal resolution, are spectrally similar and can hence be regarded as a “virtual constellation” (WULDER et al. 2015). If appropriate processing steps are applied, data from both satellites can be used in conjunction. Here, the *Framework for Operational Radiometric Correction for Environmental monitoring* (FORCE) was used to ensure this appropriate processing (FRANTZ 2019). FORCE applies a consistent processing scheme to both Landsat and Sentinel-2 (FRANTZ et al. 2016). This includes the radiometric correction and harmonization of the data as well as the generation of quality flags to remove pixels covered by clouds, cloud shadows, snow, etc. Thereby, the software uses a modified version of the popular Fmask algorithm (ZHU & WOODCOCK 2012) that considers parallax effects in the Sentinel-2 imagery to overcome the lack of a thermal band of this satellite (FRANTZ et al. 2018). Using the same software, the spatial characteristics of both types of data were aligned, i.e. all data were projected into one common coordinate system, resampled to the same resolution of 10 m, and subdivided into tiles of  $30 \times 30$  km. As the study area fits in one of these tiles, all other tiles were disregarded to reduce data volume.

Likewise, Sentinel-1 was processed extensively as well data as well, whereby the majority of processing was performed on the Google Earth Engine cloud processing platform (GORELICK et al. 2017). The Sentinel-1 GRD imagery available on this platform is already preprocessed, including thermal noise removal, radiometric calibration, and terrain correction. This data was further processed using one consistent workflow (MULLISSA et al. 2021). Specifically, a border noise correction was applied, as well as a multitemporal Quegan speckle filter. To account for terrain and use both ascending and descending Sentinel-1 orbits in conjunction, radiometric terrain flattening was applied as well (VOLLRATH et al. 2020). The processed data was exported from Google Earth Engine, and using the FORCE software again, its spatial characteristics were aligned with Landsat and Sentinel-2. Thereby one consistent data cube of all available Landsat, Sentinel-2, and Sentinel-1 images, with a spatial resolution of 10 m, was created. A total of 25 parameters were computed from this data, including 10 “traditional” vegetation indices, 11 indices based on Sentinel 2’s red edge channels, and 4 SAR parameters from Sentinel-1. An overview of the parameters is listed in Table 1. To remove seasonal fluctuations and noise from the data, every time series of every index in every pixel were smoothed using locally estimated Scatterplot Smoothing (LOESS) models. LOESS is an implementation of local regression (HASTIE et al. 2009).

### 2.3.2 Sampling and Class Separability Assessment

The fitting of the detection algorithm implemented in this study requires data representing both healthy and disturbed forests. This data was gathered with the reference dataset mentioned above. Yearly median composites for the years 2014 to 2018 were computed for all 25 parameters, and these were sampled according to the following strategy: to gain data representing disturbed forests,

these composites were sampled with the reference data of the previous year. Vice-versa, composites were sampled with the reference data of two years afterwards to gain data representing healthy forests. E.g. the median composite of 2017 was sampled with areas that were subject to bark beetle infestations in the year before to ensure that the sampled values definitely represent infested forests. The same composite was also sampled with areas that were infested in 2019 based on the assumption that forests infested in this year had still been healthy in 2017. To assess which of the 25 parameters separate healthy and infested forests best, the Jeffries-Matusita (JM) distance was computed for any of them. This measure has a finite range of 0 to 2, with 0 indicating complete inseparability and 2 indicating full separability (LALIBERTE et al. 2012). The multispectral parameter  $v1$  and SAR parameter  $v2$  with the highest separability, respectively, were selected for further analysis.

### 2.3.3 Disturbance Detection

Disturbances were detected for all pixels that were subject to bark beetle infestations in 2019 as well as an equal number of pixels that were known to be still healthy during this year. To detect disturbances, a Bayesian approach was applied (REICHE et al. 2018, 2015). From the distributions of the sampled values for the two best-performing variables, Gaussian probability density functions were computed, and the probability densities  $p(v1|H)$  and  $p(v2|H)$  that a pixel belongs to a healthy forest as well as densities  $p(v1|I)$  and  $p(v2|I)$  that it belongs to an infested forest were computed. From these, the conditional probability of an infestation could be derived using Bayes' theorem (MCELREATH 2020), assuming equal priors for healthy and infested:

$$P(I|v1_t) = \frac{p(v1_t|I)}{p(v1_t|I) + p(v1_t|H)} \text{ for } t \in T_{v1} \quad (1)$$

where  $t$  is the date in the time series of a given satellite observation (REICHE et al. 2015). Analogously, the parameter time series of both selected variables for every pixel were transformed into infestation probability time series. This procedure is illustrated for one example pixel in Fig. 2. The detection itself was performed by binarily classifying the time series into healthy and infested using 100 increasing probability thresholds between 0.01 and 1. Thereby, the detection capabilities of five different sensor configurations were examined:

- Multispectral, i.e. all observations of  $P(I|v1_t)$ .
- Landsat, i.e.  $P(I|v1_t)$  with a subset of  $t$  corresponding to the Landsat observation dates.
- Sentinel-2, i.e.  $P(I|v1_t)$  with a subset of  $t$  representing the Sentinel-2 observation dates.
- Sentinel-1, i.e. all observations of  $P(I|v2_t)$ .
- Fused, i.e.  $P(I|v1_t)$  and  $P(I|v2_t)$  combined, arranged by  $t$ .

By comparison to areas in the national park that were still healthy and pixels that were infested in 2019, the spatial accuracy of detections was assessed. If a pixel was detected as infested under a given threshold, the date of the satellite observation during which the detection occurred was recorded. Infestations that were recorded before April 1<sup>st</sup>, 2019 (the approximate beginning of the bark beetle season) were regarded as false detections and consequently not counted. The same holds true for observations detected later than September 30<sup>th</sup>, 2020 (one year after the approximate end of the bark beetle season in 2019). Besides, to increase confidence in the results, only

detections were counted that were confirmed by two additional observations that were higher than the applied threshold. The overall spatial accuracies, omission and commission error of the infested class, and summary statistics on the detection date were computed.

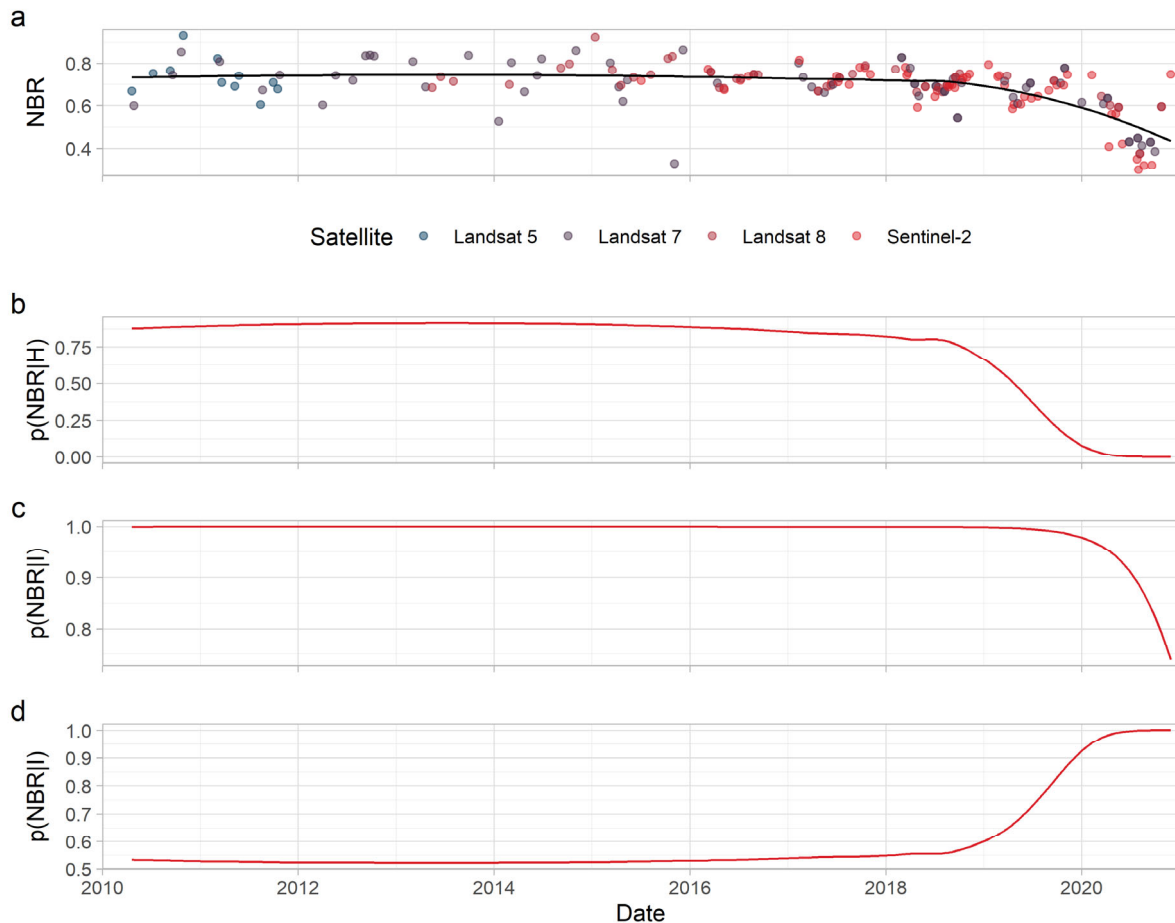


Fig. 2: Illustration of the derivation of infestation probabilities for one random example pixel infested in 2019, for the Multispectral sensor configuration. a) the original NBR time series. Colors indicate the satellite of the respective observation, the black line is the LOESS-smoothed time series. b) the derived healthy probabilities, c) the derived infested probabilities, d) conditional probabilities of an infestation

### 3 Results and Discussion

Fig. 3 depicts the results of the class separability according to the JM distance. The Normalized Difference Burn Ratio (NBR) was the parameter with the highest separability, scoring a Jeffries-Matusita Distance of 1.6 on a scale of 0 to 2. In general, the NBR and other vegetation indices that incorporate the Landsat/Sentinel-2 Shortwave Infrared (SWIR) bands, i.e. the Normalized Difference Moisture Index (NDM) and Normalized Difference Tillage Index, achieved the best results, as did some Sentinel-2 red-edge indices. This is in line with existing literature documenting the sensitivity of SWIR bands of Landsat and Sentinel-2, as well as the red edge region of the electromagnetic spectrum, to physiological changes in trees induced by bark beetle disturbances

(ABDULLAH et al. 2018; GOODWIN et al. 2008; MEIGS et al. 2011). Other parameters performed considerably worse, especially the SAR-based metrics, all of which achieved JM distance values below 0.5. Thereby, the VV band offered the relative highest separability (Jeffries-Matusita Distance of 0.3) of all four SAR parameters. According to the methodology described above, the NBR and the VV backscatter were selected as  $v1$  and  $v2$  for the detection.

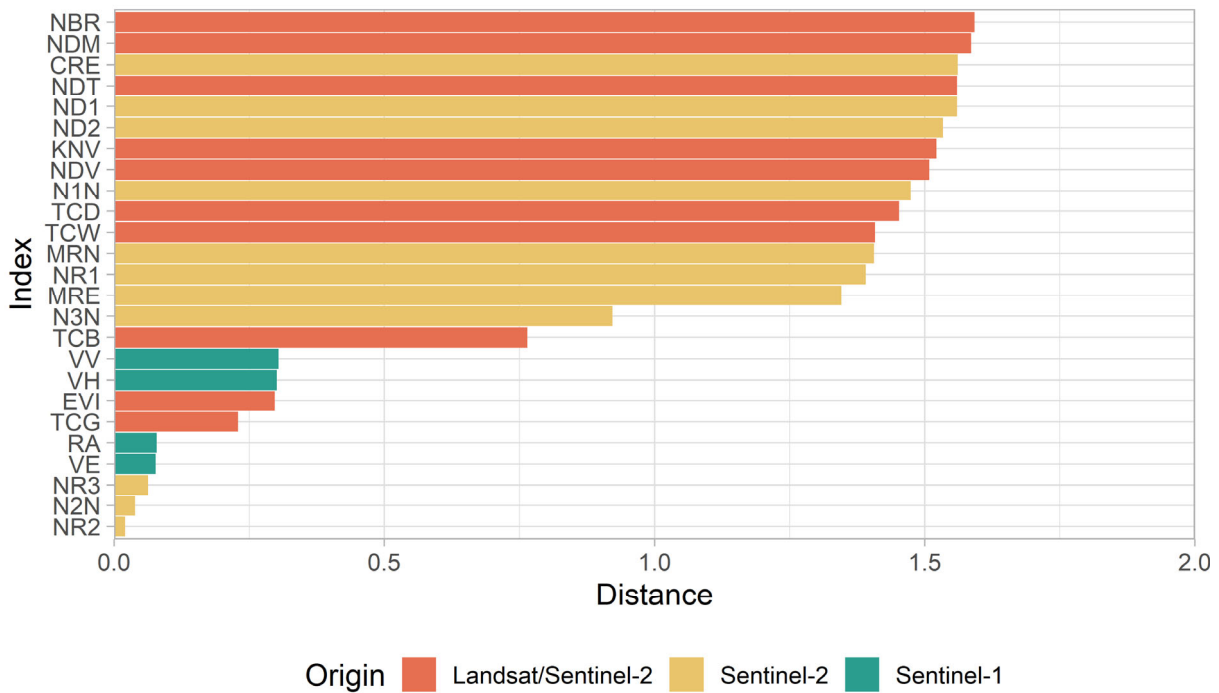


Fig. 3: Jeffries-Matusita Distance for all 25 computed parameters. Colors represent the origin of the parameter

Fig. 4 shows the overall spatial accuracies of the five different sensor configurations, depending on the applied thresholds, together with the corresponding omission and commission errors. Here, Sentinel-2 achieved the best results, with a maximum overall accuracy of 0.86 at a probability threshold of 0.9. Landsat and the combination of Landsat and Sentinel-2 achieved somewhat inferior results, whereby both sensor configurations are highly similar. The commission errors for Sentinel-2 are slightly higher, but this is more than compensated by the lower omission errors, making Sentinel-2 the best-performing sensor configuration. Sentinel-1 and the combination of all sensors by comparison perform much worse. While the maximum overall accuracies of the all-sensor configuration are still relatively good for some of the thresholds, Sentinel-1 only barely reaches a maximum overall accuracy of 0.55, and for lower probability thresholds, the overall accuracy is 0.5 (i.e. as good as a random classifier). This is the case because – while commission errors are comparably low, the omission errors are very high, i.e. 100 % for thresholds < 0.25. This means that in general, very few disturbances are detected at all by both sensor configurations. Since the better-performing multispectral data is included as well, the fusion configuration based on all datasets exhibits somewhat lower omission errors at least for thresholds > 0.5

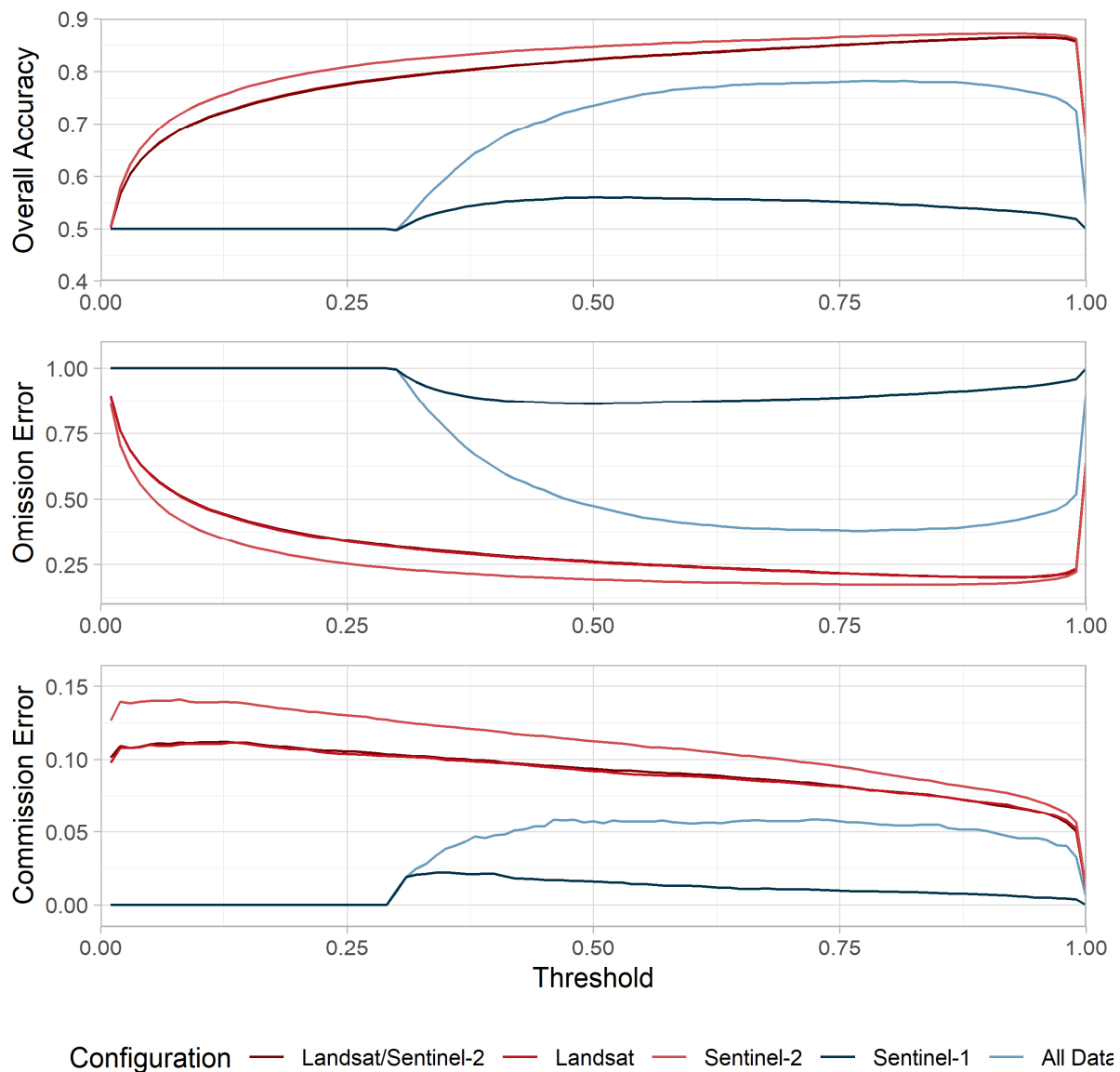


Fig. 4: Overall accuracies (top) as well as omission (center) and commission errors (bottom) for the infested class, according to the applied probability threshold. Colors represent the five sensor configurations

If the date of detection is compared between Landsat, Sentinel-2, and their combination for the respective threshold of highest spatial accuracy (Fig. 5), Sentinel-2 is at an advantage here as well. The median detection date of Sentinel-2 is nearly 1 month earlier compared to Landsat and the combination of both, whereby the two latter sensor configurations achieve very similar results once again. A detailed assessment of the time it takes from an infestation in the field to be detected by the applied satellite configurations was not possible, because the reference dataset only documents the year of an infestation, but not the infestation date at a sub-annual level. Yet, the fact that Sentinel-2 on average detects the same infestations one month earlier than Landsat or the combination of both leads to the conclusion that Sentinel-2 is indeed better equipped for an early

detection. The approach developed here allows for the choice of a threshold that suits user needs: if a lower threshold is applied, earlier detections are possible, at the price of higher errors, whereby the commission errors are generally very low and with Sentinel-2, omission errors are low as well even with relatively low thresholds (e.g. 0.25). If very high spatial accuracies ( $> 0.8$ ) are the goal, e.g. for detailed damage inventories, higher probability thresholds can be applied, even though this leads to disturbances being detected later.

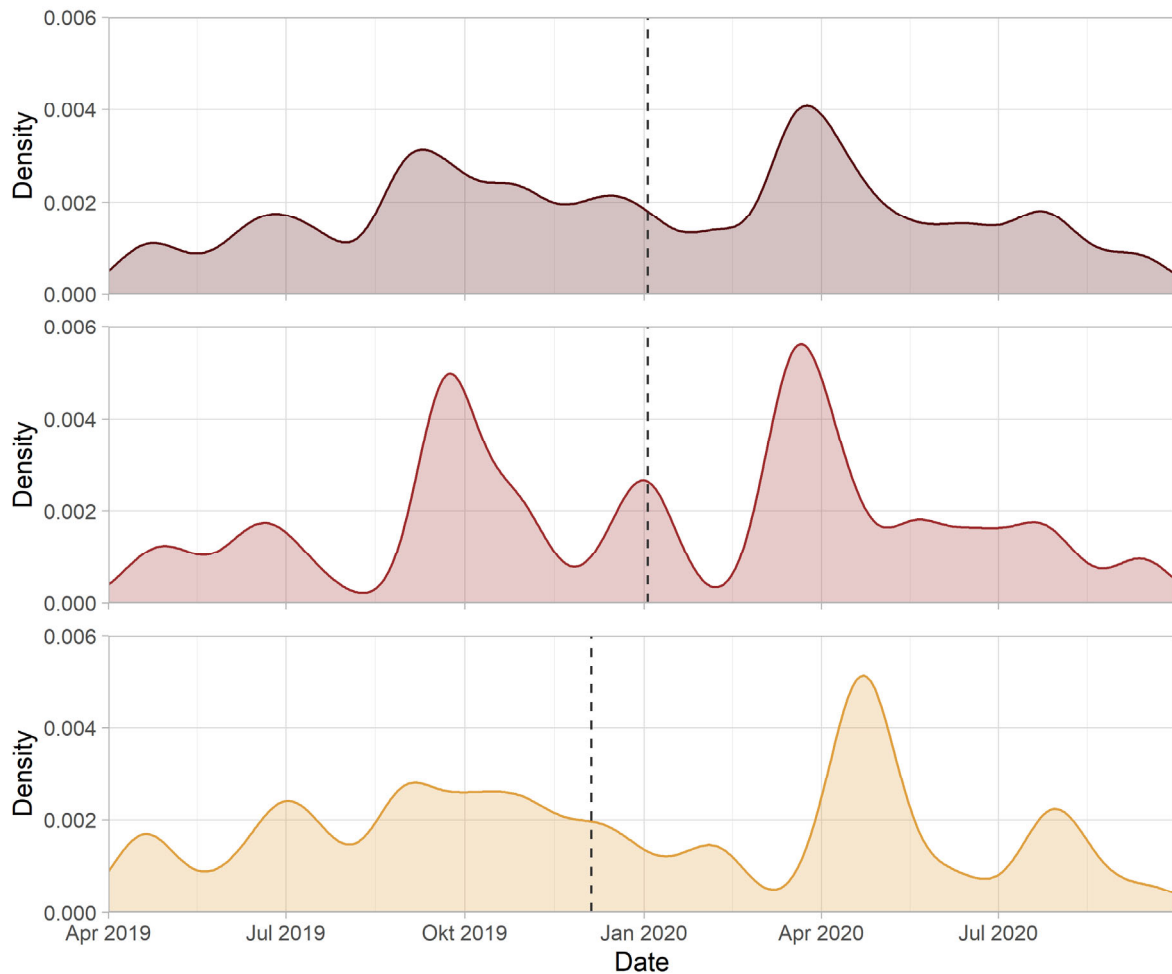


Fig. 5: Detection Dates of all pixels infested in 2017 according to the reference data. Top: Landsat and Sentinel-2 combined, center: Landsat only, bottom: Sentinel-2 only. Dashed lines represent mean detection dates

The overall good performance of Sentinel-2 can be attributed to its relatively high spatial, temporal, and spectral resolution, confirming the high potential that this satellite has for forestry applications. With similar spectral characteristics, Landsat achieves somewhat inferior results probably due to its lower spatial and temporal resolution, which also impacted the combination of both. The worse performance of the two configurations that included SAR data are likely a result of the suboptimal suitability of Sentinel-1 due to its C-band radiation not being able to penetrate forest canopy, as well as topographic and speckle effects that were not fully removed. This

however is a result of the approach applied here, relying on the automated processing of a large number of images. Possibly, more elaborate processing of fewer Sentinel-1 images and the tryout of different speckle filters may improve its results in the future.

## 4 Conclusion

This study utilized full time series of Landsat, Sentinel-2, and Sentinel-1 as well as a combination of multispectral and SAR data to detect forest disturbances induced by bark beetle infestations in the Bavarian Forest National Park, Germany. As elaborated in the results, all multispectral sensor configurations produced sensible results, with Sentinel-2 as the best-equipped satellite for the detection of bark beetle disturbances in terms of both time and space. The combination of Landsat and Sentinel-2 provided good results but is not necessary as it yields no advantage over applying Sentinel-2 alone. By comparison, using SAR data did not provide meaningful results, and neither did the combination of SAR and multispectral data. With the approach developed here, different probability thresholds can be applied for the detection, allowing potential users of an operational monitoring based on this approach to decide whether the goal is to detect infested trees very early (i.e. in Near-Realtime) or if a highly accurate inventory of disturbances is the goal. This is a key advantage of a potential monitoring tool based on this study. To conclude, the results of this study gave important insights about the usage of satellite data in the detection of bark beetle infestations. This is an important step in a better monitoring of these disturbances in Central Europe.

## 5 References

- ABDULLAH, H., DARVISHZADEH, R., SKIDMORE, A.K., GROEN, T.A. & HEURICH, M., 2018: European spruce bark beetle (*Ips typographus*, L.) green attack affects foliar reflectance and biochemical properties. *International Journal of Applied Earth Observation and Geoinformation*, **64**, 199-209. <https://doi.org/10.1016/j.jag.2017.09.009>.
- ABDULLAH, H., SKIDMORE, A.K., DARVISHZADEH, R. & HEURICH, M., 2019: Sentinel-2 accurately maps green-attack stage of European spruce bark beetle (*Ips typographus*, L.) compared with Landsat-8. *Remote Sensing in Ecology and Conservation*, **5**, 87-106. <https://doi.org/10.1002/rse2.93>.
- BÁRTA, V., LUKEŠ, P. & HOMOLOVÁ, L., 2021: Early detection of bark beetle infestation in Norway spruce forests of Central Europe using Sentinel-2. *International Journal of Applied Earth Observation and Geoinformation*, **100**, 102335. <https://doi.org/10.1016/j.jag.2021.102335>.
- BROCKERHOFF, E.G., BARBARO, L., CASTAGNEYROL, B., FORRESTER, D.I., GARDINER, B., GONZÁLEZ-OLABARRIA, J.R., LYVER, P.O., MEURISSE, N., OXBROUGH, A., TAKI, H., THOMPSON, I.D., VAN DER PLAS, F. & JACTEL, H., 2017: Forest biodiversity, ecosystem functioning and the provision of ecosystem services. *Biodiversity and Conservation*, **26**, 3005-3035. <https://doi.org/10.1007/s10531-017-1453-2>.
- BUNDESMINISTERIUM FÜR ERNÄHRUNG UND LANDWIRTSCHAFT, 2021: Waldbericht der Bundesregierung 2021. Bonn.
- FRANTZ, D., 2019: FORCE—Landsat + Sentinel-2 Analysis Ready Data and Beyond. *Remote Sensing*, **11**, 1124. <https://doi.org/10.3390/rs11091124>.

- FRANTZ, D., HAß, E., UHL, A., STOFFELS, J. & HILL, J., 2018: Improvement of the Fmask algorithm for Sentinel-2 images: Separating clouds from bright surfaces based on parallax effects. *Remote Sensing of Environment*, **215**, 471-481. <https://doi.org/10.1016/j.rse.2018.04.046>.
- FRANTZ, D., RÖDER, A., STELLMES, M. & HILL, J., 2016: An Operational Radiometric Landsat Preprocessing Framework for Large-Area Time Series Applications. *IEEE Transactions on Geoscience and Remote Sensing*, **54**, 3928-3943. <https://doi.org/10.1109/TGRS.2016.2530856>.
- GOODWIN, N.R., COOPS, N.C., WULDER, M.A., GILLANDERS, S., SCHROEDER, T.A. & NELSON, T., 2008: Estimation of insect infestation dynamics using a temporal sequence of Landsat data. *Remote Sensing of Environment*, **112**, 3680-3689. <https://doi.org/10.1016/j.rse.2008.05.005>.
- GORELICK, N., HANCHER, M., DIXON, M., ILYUSHCHENKO, S., THAU, D. & MOORE, R., 2017: Google Earth Engine: Planetary-scale geospatial analysis for everyone. *Remote Sensing of Environment*, **202**, 18-27. <https://doi.org/10.1016/j.rse.2017.06.031>.
- HAIŠ, M. & KUČERA, T., 2008: Surface temperature change of spruce forest as a result of bark beetle attack: remote sensing and GIS approach. *European Journal of Forest Research*, **127**, 327-336. <https://doi.org/10.1007/s10342-008-0208-8>.
- HASTIE, T., TIBSHIRANI, R. & FRIEDMAN, J.H., 2009: *The elements of statistical learning: data mining, inference, and prediction*, 2nd ed. Springer, New York.
- HEURICH, M., BEUDERT, B., RALL, H. & KŘENOVÁ, Z., 2010: National Parks as Model Regions for Interdisciplinary Long-Term Ecological Research: The Bavarian Forest and Šumavá National Parks Underway to Transboundary Ecosystem Research, Long-Term Ecological Research: Between Theory and Application. Müller, F., Baessler, C., Schubert, H., Klotz, S. (Eds.), Springer Netherlands, Dordrecht, 327-344. [https://doi.org/10.1007/978-90-481-8782-9\\_23](https://doi.org/10.1007/978-90-481-8782-9_23).
- HLÁSNY, T., KÖNIG, L., KROKENE, P., LINDNER, M., MONTAGNÉ-HUCK, C., MÜLLER, J., QIN, H., RAFFA, K.F., SCHELHAAS, M.-J., SVOBODA, M., VIIRI, H. & SEIDL, R., 2021: Bark Beetle Outbreaks in Europe: State of Knowledge and Ways Forward for Management. *Current Forestry Reports*, **7**, 138-165. <https://doi.org/10.1007/s40725-021-00142-x>.
- HOLLAUS, M. & VREUGDENHIL, M., 2019: Radar Satellite Imagery for Detecting Bark Beetle Outbreaks in Forests. *Current Forestry Reports*, **5**, 240-250. <https://doi.org/10.1007/s40725-019-00098-z>.
- HUO, L., PERSSON, H.J. & LINDBERG, E., 2021: Early detection of forest stress from European spruce bark beetle attack, and a new vegetation index: Normalized distance red & SWIR (NDRS). *Remote Sensing of Environment*, **255**, 112240. <https://doi.org/10.1016/j.rse.2020.112240>
- LALIBERTE, A.S., BROWNING, D.M. & RANGO, A., 2012: A comparison of three feature selection methods for object-based classification of sub-decimeter resolution UltraCam-L imagery. *International Journal of Applied Earth Observation and Geoinformation*, **15**, 70-78. <https://doi.org/10.1016/j.jag.2011.05.011>.
- LATIFI, H., HOLZWARTH, S., SKIDMORE, A., BRŮNA, J., ČERVENKA, J., DARVISHZADEH, R., HAIŠ, M., HEIDEN, U., HOMOLOVÁ, L., KRZYSZEK, P., SCHNEIDER, T., STARÝ, M., WANG, T., MÜLLER, J. & HEURICH, M., 2021: A laboratory for conceiving Essential Biodiversity

- Variables (EBVs)—The ‘Data pool initiative for the Bohemian Forest Ecosystem.’ *Methods in Ecology and Evolution*, **12**, 2073-2083. <https://doi.org/10.1111/2041-210X.13695>.
- MCÉLREATH, R., 2020: *Statistical rethinking: A Bayesian course with examples in R and Stan*, 2nd ed. Taylor and Francis, CRC Press, Boca Raton.
- MEIGS, G.W., KENNEDY, R.E. & COHEN, W.B., 2011: A Landsat time series approach to characterize bark beetle and defoliator impacts on tree mortality and surface fuels in conifer forests. *Remote Sensing of Environment*, **115**, 3707–3718. <https://doi.org/10.1016/j.rse.2011.09.009>.
- MILLAR, C.I. & STEPHENSON, N.L., 2015: Temperate forest health in an era of emerging megadisturbance. *Science*, **349**, 823-826. <https://doi.org/10.1126/science.aaa9933>.
- MULLISSA, A., VOLLRATH, A., ODONGO-BRAUN, C., SLAGTER, B., BALLING, J., GOU, Y., GORELICK, N. & REICHE, J., 2021: Sentinel-1 SAR Backscatter Analysis Ready Data Preparation in Google Earth Engine. *Remote Sensing*, **13**, 1954. <https://doi.org/10.3390/rs13101954>.
- REICHE, J., DE BRUIN, S., HOEKMAN, D., VERBESSELT, J. & HEROLD, M., 2015: A Bayesian Approach to Combine Landsat and ALOS PALSAR Time Series for Near Real-Time Deforestation Detection. *Remote Sensing*, **7**, 4973-4996. <https://doi.org/10.3390/rs70504973>.
- REICHE, J., HAMUNYELA, E., VERBESSELT, J., HOEKMAN, D. & HEROLD, M., 2018: Improving near-real time deforestation monitoring in tropical dry forests by combining dense Sentinel-1 time series with Landsat and ALOS-2 PALSAR-2. *Remote Sensing of Environment*, **204**, 147-161. <https://doi.org/10.1016/j.rse.2017.10.034>.
- SEIDL, R., THOM, D., KAUTZ, M., MARTIN-BENITO, D., PELTONIEMI, M., VACCHIANO, G., WILD, J., ASCOLI, D., PETR, M., HONKANIEMI, J., LEXER, M.J., TROTSIUK, V., MAIROTA, P., SVOBODA, M., FABRIKA, M., NAGEL, T.A. & REYER, C.P.O., 2017: Forest disturbances under climate change. *Nature Climate Change*, **7**, 395-402. <https://doi.org/10.1038/nclimate3303>.
- SENF, C., SEIDL, R. & HOSTERT, P., 2017: Remote sensing of forest insect disturbances: Current state and future directions. *International Journal of Applied Earth Observation and Geoinformation* **60**, 49-60. <https://doi.org/10.1016/j.jag.2017.04.004>.
- VOLLRATH, A., MULLISSA, A. & REICHE, J., 2020: Angular-Based Radiometric Slope Correction for Sentinel-1 on Google Earth Engine. *Remote Sensing*, **12**, 1867. <https://doi.org/10.3390/rs12111867>.
- WULDER, M.A., DYMOND, C.C., WHITE, J.C., LECKIE, D.G. & CARROLL, A.L., 2006: Surveying mountain pine beetle damage of forests: A review of remote sensing opportunities. *Forest Ecology and Management*, **221**, 27-41. <https://doi.org/10.1016/j.foreco.2005.09.021>.
- WULDER, M.A., HILKER, T., WHITE, J.C., COOPS, N.C., MASEK, J.G., PFLUGMACHER, D. & CREVIER, Y., 2015: Virtual constellations for global terrestrial monitoring. *Remote Sensing of Environment*, **170**, 62-76. <https://doi.org/10.1016/j.rse.2015.09.001>.
- ZHU, Z. & WOODCOCK, C.E., 2012: Object-based cloud and cloud shadow detection in Landsat imagery. *Remote Sensing of Environment*, **118**, 83-94. <https://doi.org/10.1016/j.rse.2011.10.028>.